ISSN: 2689-1204

Research Article

Journal of Applied Material Science & Engineering Research

Analysis of Nonlocality, Surface Energy, and Initial Stress on the Dynamic Behaviour of Carbon Nanotubes Conveying Fluid Resting on Elastic Foundations in a Thermo-Magnetic Environment using Variation of Parameter Method

Gbeminiyi M Sobamowo*, Olorunfemi O Isaac, Suraju A Oladosu, Rafiu O Kuku

Department of Mechanical Engineering, Lagos State University, Nigeria

***Corresponding Author**
Gbeminiyi M Sobamowo, Department of Mechanical Engineering, University of Lagos, Nigeria

Submitted: 2023, Mar 27; **Accepted:** 2023, Apr 13; **Published:** 2023, May 04

Citation: Sobamowo. G., M. Isaac, O. O., Oladosu, S. A., Kuku, R. O. (2023). Analysis of Nonlocality, Surface Energy, and Initial Stress on the Dynamic Behaviour of Carbon Nanotubes Conveying Fluid Resting on Elastic Foundations in a Thermo-Magnetic Environment using Variation of Parameter Method. *J App Mat Sci & Engg Res, 7*(1), 29-42.

Abstract

This work analyzes the simultaneous impacts of surface elasticity, initial stress, residual surface tension and nonlocality on the nonlinear vibration of single-walled carbon conveying nanotube resting on linear and nonlinear elastic foundation and operating in a thermo-magnetic environment. Equation of motion governing the vibration of the nanotube was derived using Erigen's theory, Euler-Bernoulli's theory and Hamilton's principle. The partial differential equation was converted to ordinary differential equation using Galerkin's decomposition method and the ordinary differential equation was solved with the aid of variation of parameter method. Through the parametric studies, it was revealed that the ratio of the nonlinear to linear frequencies increases with the negative value of the surface stress while it decreases with the positive value of the surface stress. At any given value of nonlocal parameters, the surface effect reduces for increasing in the length of the nanotube. ratio of the frequencies decreases with increase in the strength of the magnetic field, nonlocal parameter and the length of the nanotube. The natural frequency of the nanotube gradually approaches the nonlinear Euler–Bernoulli beam limit at high values of nonlocal parameter and nanotube length. nonlocal parameter reduces the surface effects on the ratio of the frequencies. Increase in temperature change at high temperature causes decrease in the frequency ratio. However, at room or low temperature, the frequency ratio of the hybrid nanostructure increases as the temperature change increases. Also, the ratio of the frequencies at low temperatures is lower than at high temperatures. The present work will assist in the control and design of carbon nanotubes operating in thermo-magnetic environment and resting on elastic foundations.

Keywords: Surface Effects; Carbon nanotubes; Nonlocal elasticity theory; variation of parameter method.

1. Introduction

Iijima [1] discovered nanostructures discovered which has led to production of carbon nanotubes that have been widely utilized for medical, industrial, electrical, thermal, electronic and mechanical applications [2-5]. Although, some studies have been put forward on the vibrations analysis of the structures [6-13], the effects of the surface energy and initial stress are neglected in the studies. Indisputably, the properties of the region of the solid surface are different properties from the bulk material. Also, for classical structures, surface energy-to-bulk energy ratio is small. However, nanostructures have large surface energy-to-bulk energy ratio and high ratio of surface energies to volume, elastic modulus and mechanical strength. Consequently, the mechanical behaviours, bending deformation and elastic waves of the nanostructures are greatly influenced. Therefore, the surface energy effects cannot be neglected in the dynamic behaviour analysis of nanostructures. Such surface energy of nanostructures is composed of the surface tension and surface modulus exerted on the surface layer of nanostructures [13-20]. Using nonlocal elasticity theory, Wang [13] analyzed surface effects on the vibration behaviour of carbon nanotubes. Few years later, Zhang and Meguid [14] presented the impacts of surface energy on the dynamic behaviour and instability of nanobeams conveying fluids. Hosseini et al. [15] studied the influence of surface energy on the nonlocal instability of cantilever piezoelectric carbon nanotubes conveying fluid. The combined effects of surface energy and nonlocality on the flutter instability of cantilevered nanotubes conveying fluid under the influence of follower forces were explored by Bahaadini et al. [16]. Using nonlocal elasticity theory, Wang and Feng [17,18] investigated the effects of the surface stress on contact problems at nanoscale and proposed a theoretical model considering the joint effects of the elastic modulus of the surface and residual stress for vibration analysis on the basis of Euler-Bernoulli beam model. Farshi [19] explored the surface effect on vibration behaviour of single-walled carbon nanotube while Lee and Chang [20, 21] confirmed the surface effect plays a significant role on vibration frequency of nano-beam through the Rayleigh-Ritz method. Other researchers [22-28] also examined the significance of surface stress and energy on the dynamic response and instability of nanostructures.

Carbon nanotubes often suffer from initial stresses due to residual stress, thermal effects, surface effects, mismatches between the material properties of CNTs and surrounding mediums, initial external loads and other physical issues. The effects of initial stress on the dynamic behaviour of nanotubes have been studied [29-37]. However, because of their significant in practically nano-apparatus applications, there is a need for a combined on the effects of surface behaviours, initial stress and nonlocality on the physical characteristics and mechanical behaviours of carbon nanotubes. Also, scanning through the past works and to the best of the authors' knowledge, a study on simultaneous effects of surface energy and initial stress on the vibration characteristics of nanotubes resting of Winkler and Pasternak foundations in a thermo-magnetic environment has not been carried out.

In the past and recent studies, different numerical and analytical approximate methods have been adopted to analyze the nonlinearity in vibration problems. Such studies of using approximate analytical methods have been largely based on the applications homotopy analysis method (HAM), Adomain decomposition method (ADM), differential transformation method (DTM), variational iteration method (VIM), variation of parameter method (VPM), optimal homotopy asymptotic method (OHAM) etc. However, the determination of the included unknowns (that will satisfy the second boundary conditions) accompanying the approximate analytical solutions of these methods in analyzing the nonlinear problems increases the computational cost and time. Further, numerical schemes are used for the determination of the unknown included parameters. Practically, this attests that the methods (HAM, ADM, VIM, VPM, DTM, OHAM, DJM, and TAM) can be classified as semi-analytical methods rather than pure approximate analytical methods such as regular, singular and homotopy perturbation methods. Also, these methods (HAM, ADM, VIM, VPM, DTM, OHAM, DJM and TAM) traded off relative simplicity and low computational cost for high accuracy as compared to the perturbation methods. Indisputably, the use of relatively simple, low cost and accurate method is still required in analysing the process and nonlinear equations.

Variation of parameter method (VPM) for solving linear and nonlinear differential equations has fast gained ground as it appeared in many engineering and scientific research papers. It is an approximate analytical method that could solve differential equations, difference equation, differential-difference equations, fractional differential equation, pantograph equation and integro-differential equation. It solves nonlinear integral and differential equations without linearization, discretization, closure, restrictive assumptions, perturbation, approximations, round-off error and discretization that could result in massive numerical computations. It reduces complexity of expansion of derivatives and the computational difficulties of the other traditional approximation analytical or perturbation methods. It provides excellent approximations to the solution of non-linear equation with high accuracy. Moreover, the need for small perturbation parameter as required in traditional PMs, the rigour of the derivations of differential transformations or recursive relation as carried out in DTM, the difficulty in determining the Adomian polynomials as in ADM, the restrictions of HPM to weakly nonlinear problems as established in literatures, the lack of rigorous theories or proper guidance for choosing initial approximation, auxiliary linear operators, auxiliary functions, auxiliary parameters, and the requirements of conformity of the solution to the rule of coefficient ergodicity as done in HAM, the search Langrange multiplier as carried in VIM, and the challenges associated with proper construction of the approximating functions for arbitrary domains or geometry of interest as in Galerkin weighted residual method (GWRM), least square method (LSM) and collocation method (CM) are some of the difficulties that VPM overcomes. Additionally, the review of past works has shown that VPM has not been adopted to solve the nonlinear problem. Therefore, in this present study, the coupled impacts of surface effects, initial stress and nonlocality on the nonlinear dynamic behaviour of single-walled carbon nanotubes resting on Winkler (Spring) and Pasternak (Shear layer) foundations in a thermal-magnetic environment. Erigen's nonlocal elasticity [38-39], Maxwell's relations, Hamilton's principle, surface effect and Euler-Bernoulli beam theories are adopted to develop the systems of nonlinear equations of the dynamics behaviour of the carbon nanotube. The partial differential equation was converted to ordinary differential equation using Galerkin's decomposition method and the ordinary differential equation was solved with the aid of variation of parameter method. Although, the study is majorly directed to analyze the impacts of surface, nonlocality and initial stress on the vibration of the nanostructures, it is known that magnetic field and temperature change/gradients can significantly change the vibration characteristics of nanotubes as they affect the homogeneous nanotubes.

2. Model Development

Consider a single-walled CNT of length L and inner and outer diameters D_i and D_o resting on Winkler (Spring) and Pasternak (Shear layer) foundations as illustrated in Fig. 1. The SWCNTs conveying a hot fluid and resting on elastic foundation under external applied tension, initial stress, magnetic and temperature fields as shown in the figure.

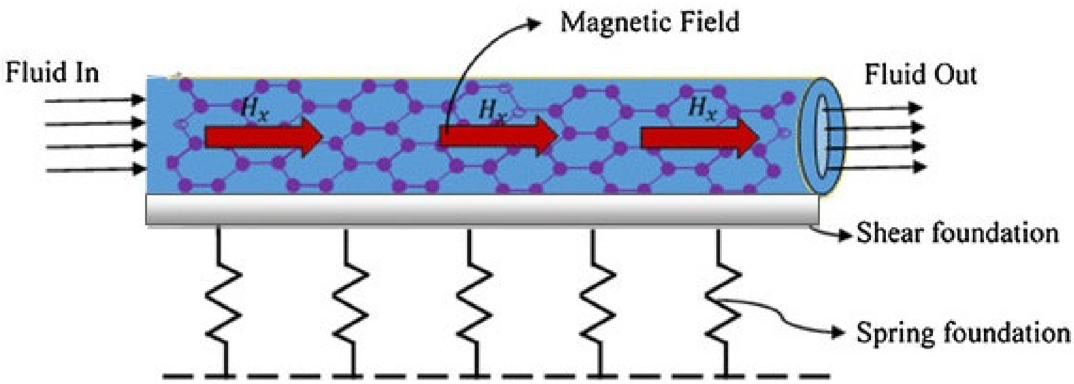

Figure 1: Carbon nanotube conveying hot fluid resting on elastic foundation

2.1 Nonlocal elasticity theory

Based on the nonlocal elasticity theory and given considerations to the nonlocal effects of higher-order strain gradients, the differential relations involving the stress resultants and the strains for the nanotube:

$$\sigma_{xx} - (e_0 a)^2 \frac{\partial^2 \sigma_{xx}}{\partial x^2} = E\varepsilon_{xx} \tag{1}$$

The strain–displacement relation,

$$\varepsilon_{xx} = -z\frac{\partial^2 w(x,t)}{\partial x^2} \tag{2}$$

In case of small deformation, the strain strain–displacement relation

$$\varepsilon_{xx} = -z\frac{\partial^2 w}{\partial x^2} \tag{3}$$

Therefore,

$$\sigma_{xx} - (e_0 a)^2 \frac{\partial^2 \sigma_{xx}}{\partial x^2} = -Ez\frac{\partial^2 w}{\partial x^2} \tag{4}$$

Multiply Eq. (4) through by *zdA*

$$\sigma_{xx} zdA - (e_0 a)^2 \frac{\partial^2 (z\sigma_{xx})}{\partial x^2} dA = -Ez^2 \frac{\partial^2 w}{\partial x^2} dA \tag{5}$$

On integrating both sides of Eq. (8), we have

$$\int_A \sigma_{xx} zdA - (e_0 a)^2 \frac{\partial^2}{\partial x^2}\int_A z\sigma_{xx} dA = -E\frac{\partial^2 w}{\partial x^2}\int_A z^2 dA \tag{6}$$

Recall that the bending moment and second moment of area of the nanotube are given as

$$M = \int_A z\sigma_{xx} dA \tag{7}$$

and

$$I = \int_A z^2 dA \tag{8}$$

Therefore, Eq. (6) can be written as

$$M - (e_0 a)^2 \frac{\partial^2 M}{\partial x^2} = -EI\frac{\partial^2 w}{\partial x^2} \tag{9}$$

The above Eq. (9) shows the relationship between the flexural displacement w and the bending moment M of the nanotube can be obtained.

If Eq. (9) is differentiated twice, we have

$$\frac{\partial^2 M}{\partial x^2} - (e_0 a)^2 \frac{\partial^2}{\partial x^2}\left(\frac{\partial^2 M}{\partial x^2}\right) = -EI\frac{\partial^4 w}{\partial x^4} \tag{10}$$

Therefore,

$$EI\frac{\partial^4 w}{\partial x^4} + \frac{\partial^2 M}{\partial x^2} - (e_0 a)^2 \frac{\partial^2}{\partial x^2}\left(\frac{\partial^2 M}{\partial x^2}\right) = 0 \tag{11}$$

If the effect of surface is considered, we have

$$(EI + E_s I_s)\frac{\partial^4 w}{\partial x^4} + \frac{\partial^2 M}{\partial x^2} - (e_0 a)^2 \frac{\partial^2}{\partial x^2}\left(\frac{\partial^2 M}{\partial x^2}\right) = 0 \tag{12}$$

From the Euler beam theory,

$$\frac{\partial^2 M}{\partial x^2} = m_{cn}\frac{\partial^2 w}{\partial t^2} + f_{fluid\ flow} - f_{initial\,stress} + f_{axial\,tension} + f_{residual\ surface\,stress} + f_{foundation} + f_{magnetic} - f_{thermal} \tag{13}$$

The axial force per unit length as a result fluid flow effect

$$f_{fluid\ flow} = m_f\frac{\partial^2 w}{\partial t^2} + m_f u^2\frac{\partial^2 w}{\partial x \partial t} + 2um_f\frac{\partial^2 w}{\partial x \partial t} \tag{14}$$

The axial force per unit length due to initial stress

$$f_{initial\,stress} = -\delta A\sigma_x^o \frac{\partial^2 w}{\partial x^2} \quad (15)$$

The axial force per unit length due to residual surface stress

$$f_{residual\;surface stress} = H_s \frac{\partial^2 w}{\partial x^2} \quad (16)$$

The axial force per unit length due to axial tension/support

$$f_{axial\,support} = \left[\frac{EA}{2L}\int_0^L \left(\frac{\partial w}{\partial x}\right)^2 dx\right]\frac{\partial^2 w}{\partial x^2} \quad (17)$$

The force per unit length due to the Winkler and Pasternak foundations is given as

$$f_{foundation} = k_1 w - k_p \frac{\partial^2 w}{\partial x^2} + k_3 w^3 \quad (18)$$

The magnetic force per unit length as a result of Lorentz force.

$$f_{magnetic} = \eta H_x^2 A \frac{\partial^2 w}{\partial x^2} \quad (19)$$

The axial force per unit length as a result of the thermal effect

$$f_{thermal} = -\frac{EA\alpha\Delta T}{1-2\nu}\frac{\partial^2 w}{\partial x^2} \quad (20)$$

Substituting Eqs. (14) – (20) into Eq. (13), we have

$$\frac{\partial^2 M}{\partial x^2} = (m_{cn}+m_f)\frac{\partial^2 w}{\partial t^2} + 2um_f\frac{\partial^2 w}{\partial x\partial t} + \left[\frac{EA}{2L}\int_0^L\left(\frac{\partial w}{\partial x}\right)^2 dx\right]\frac{\partial^2 w}{\partial x^2} + \left(m_f u^2 + \delta A\sigma_x^o - H_s - \eta H_x^2 A - k_p + \frac{EA\alpha\Delta T}{1-2\nu}\right)\frac{\partial^2 w}{\partial x^2} + k_1 w + k_3 w^3 \quad (21)$$

On putting Eq. (20) into Eq. (12), we arrived at

$$\begin{aligned}&\left(EI+E_sI_s\right)\frac{\partial^4 w}{\partial x^4} + (m_{cn}+m_f)\frac{\partial^2 w}{\partial t^2} + 2um_f\frac{\partial^2 w}{\partial x\partial t} + \left[\frac{EA}{2L}\int_0^L\left(\frac{\partial w}{\partial x}\right)^2 dx\right]\frac{\partial^2 w}{\partial x^2}\\ &+\left(m_f u^2 + \delta A\sigma_x^o - H_s - \eta H_x^2 A - k_p + \frac{EA\alpha\Delta T}{1-2\nu}\right)\frac{\partial^2 w}{\partial x^2} + k_1 w + k_3 w^3\\ &-\left(e_o a\right)^2\left[\begin{aligned}&(m_{cn}+m_f)\frac{\partial^4 w}{\partial x^2\partial t^2} + 2um_f\frac{\partial^4 w}{\partial x^3\partial t} + \left[\frac{EA}{2L}\int_0^L\left(\frac{\partial w}{\partial x}\right)^2 dx\right]\frac{\partial^4 w}{\partial x^4}\\ &+\left(m_f u^2 + \delta A\sigma_x^o - H_s - \eta H_x^2 A - k_p + \frac{EA\alpha\Delta T}{1-2\nu}\right)\frac{\partial^4 w}{\partial x^4}\\ &+k_1\frac{\partial^2 w}{\partial x^2} + 3k_3 w^2\frac{\partial^2 w}{\partial x^2} + 6k_3 w\left(\frac{\partial w}{\partial x}\right)^2\end{aligned}\right] = 0\end{aligned} \quad (22)$$

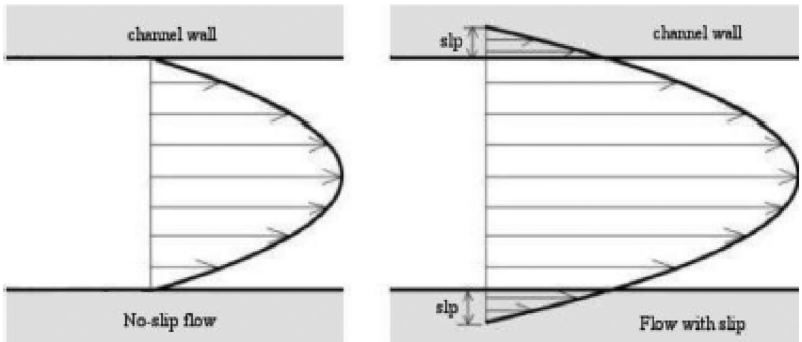

Figure 2: Effect of slip boundary condition on velocity profile [40, 41].

Fig. 2 shows the effect of flow in a channel. In the fluid-conveying carbon nanotube, the condition of slip is satisfied since in such flow, the ratio of the mean free path of the fluid molecules relative to a characteristic length of the flow geometry which is the Knudsen number is larger than 10-2. Consequently, the velocity correction factor for the slip flow velocity is proposed as [40, 41]:

$$VCF = \frac{u_{avg,slip}}{u_{avg,no-slip}} = \left(1+a_k Kn\right)\left[4\left(\frac{2-\sigma_v}{\sigma_v}\right)\left(\frac{Kn}{1+Kn}\right)+1\right] \quad (23)$$

Where Kn is the Knudsen number, σv is tangential moment accommodation coefficient which is considered to be 0.7 for most practical purposes [40, 41]

$$a_k = a_o\frac{2}{\pi}\left[tan^{-1}\left(a_1 Kn^B\right)\right] \quad (24)$$

$$a_o = \frac{64}{3\pi\left(1-\frac{4}{b}\right)} \quad (25)$$

a_1=4 and B = 0.04 and *b* is the general slip coefficient ($b = -1$).

From Eq. (23),

$$u_{avg,slip} = \left(1+a_k Kn\right)\left[4\left(\frac{2-\sigma_v}{\sigma_v}\right)\left(\frac{Kn}{1+Kn}\right)+1\right]u_{avg,no-slip} \quad (26)$$

Therefore, Eq. (22) can be written as

$$\begin{gathered}\left(EI+E_sI_s\right)\frac{\partial^4 w}{\partial x^4}+(m_{cn}+m_f)\frac{\partial^2 w}{\partial t^2}+2m_f\left(1+a_kKn\right)\left[4\left(\frac{2-\sigma_v}{\sigma_v}\right)\left(\frac{Kn}{1+Kn}\right)+1\right]\frac{\partial^2 w}{\partial x\partial t}+\left[\frac{EA}{2L}\int_0^L\left(\frac{\partial w}{\partial x}\right)^2dx\right]\frac{\partial^2 w}{\partial x^2}\\
+\left(m_f\left[\left(1+a_kKn\right)\left[4\left(\frac{2-\sigma_v}{\sigma_v}\right)\left(\frac{Kn}{1+Kn}\right)+1\right]\right]^2+\delta A\sigma_x^o-H_s-\eta H_x^2A-k_p+\frac{EA\alpha\Delta T}{1-2\nu}\right)\frac{\partial^2 w}{\partial x^2}+k_1w+k_3w^3\\
-\left(e_oa\right)^2\left[\begin{gathered}(m_{cn}+m_f)\frac{\partial^4 w}{\partial x^2\partial t^2}+2m_f\left(1+a_kKn\right)\left[4\left(\frac{2-\sigma_v}{\sigma_v}\right)\left(\frac{Kn}{1+Kn}\right)+1\right]\frac{\partial^4 w}{\partial x^3\partial t}+\left[\frac{EA}{2L}\int_0^L\left(\frac{\partial w}{\partial x}\right)^2dx\right]\frac{\partial^4 w}{\partial x^4}\\
+\left(m_f\left[\left(1+a_kKn\right)\left[4\left(\frac{2-\sigma_v}{\sigma_v}\right)\left(\frac{Kn}{1+Kn}\right)+1\right]\right]^2+\delta A\sigma_x^o-H_s-\eta H_x^2A-k_p+\frac{EA\alpha\Delta T}{1-2\nu}\right)\frac{\partial^4 w}{\partial x^4}\\
+k_1\frac{\partial^2 w}{\partial x^2}+3k_3w^2\frac{\partial^2 w}{\partial x^2}+6k_3w\left(\frac{\partial w}{\partial x}\right)^2\end{gathered}\right]=0\end{gathered}$$

(27)

where the transverse area and the bending rigidity are given as

$$A=\pi dh$$

$$EI=\frac{\pi d^3h}{8}$$

and

$$E_sI_s=\frac{\pi E_sh(d_o^3+d_i^3)}{8}$$

$$H_s=2\tau_s\left(d_o+d_i\right)$$

The symbol H_s is the parameter induced by the residual surface stress. τ is the residual surface tension, *d* and *h* are the nanotube internal diameter and thickness, respectively. It should be noted that the diameter of the nanotube can be derived from chirality indices (*n, m*)

$$d_i=\frac{a\sqrt{3}}{\pi}\sqrt{n^2+mn+m^2} \tag{28}$$

where $a\sqrt{3}=0.246\,nm$. "a" represents the length of the carbon-carbon bond. d is the inner diameter of the nanotube.

3. Analytical Solutions of Nonlinear Model of Free Vibration of the Nanotube

The nonlinear term in model in Eq. (27) makes it very difficult to provide closed-form solution to the problem. Therefore, recourse is made to homotopy perturbation to solve the nonlinear model. In order to develop analytical solutions for the developed nonlinear model, the partial differential equation is converted to ordinary differential equation using the Galerkin's decomposition procedure to decompose the spatial and temporal parts of the lateral displacement functions as

$$w(x,t)=\phi(x)u(t) \tag{29}$$

Where the generalized coordinate of the system and is a trial/comparison function that will satisfy both the geometric and natural boundary conditions.

Applying one-parameter Galerkin's solution given in Eq. (29) to Eq. (27)

$$\int_0^L R\left(x,t\right)\phi\left(x\right)dx \tag{30}$$

where

$$R(x,t)=(EI+E_sI_s)\frac{\partial^4 w}{\partial x^4}+(m_{cn}+m_f)\frac{\partial^2 w}{\partial t^2}+2m_f(1+a_kKn)\left[4\left(\frac{2-\sigma_v}{\sigma_v}\right)\left(\frac{Kn}{1+Kn}\right)+1\right]\frac{\partial^2 w}{\partial x\partial t}+\left[\frac{EA}{2L}\int_0^L\left(\frac{\partial w}{\partial x}\right)^2dx\right]\frac{\partial^2 w}{\partial x^2}$$

$$+\left(m_f\left[(1+a_kKn)\left[4\left(\frac{2-\sigma_v}{\sigma_v}\right)\left(\frac{Kn}{1+Kn}\right)+1\right]\right]^2+\delta A\sigma_x^o-H_s-\eta H_x^2A-k_p+\frac{EA\alpha\Delta T}{1-2\nu}\right)\frac{\partial^2 w}{\partial x^2}+k_1w+k_3w^3$$

$$-(e_oa)^2\left[\begin{array}{l}(m_{cn}+m_f)\dfrac{\partial^4 w}{\partial x^2\partial t^2}+2m_f(1+a_kKn)\left[4\left(\dfrac{2-\sigma_v}{\sigma_v}\right)\left(\dfrac{Kn}{1+Kn}\right)+1\right]\dfrac{\partial^4 w}{\partial x^3\partial t}+\left[\dfrac{EA}{2L}\displaystyle\int_0^L\left(\dfrac{\partial w}{\partial x}\right)^2dx\right]\dfrac{\partial^4 w}{\partial x^4}\\+\left(m_f\left[(1+a_kKn)\left[4\left(\dfrac{2-\sigma_v}{\sigma_v}\right)\left(\dfrac{Kn}{1+Kn}\right)+1\right]\right]^2+\delta A\sigma_x^o-H_s-\eta H_x^2A-k_p+\dfrac{EA\alpha\Delta T}{1-2\nu}\right)\dfrac{\partial^4 w}{\partial x^4}\\+k_1\dfrac{\partial^2 w}{\partial x^2}+3k_3w^2\dfrac{\partial^2 w}{\partial x^2}+6k_3w\left(\dfrac{\partial w}{\partial x}\right)^2\end{array}\right]=0$$

We have the nonlinear vibration equation of the pipe as

$$M\ddot{u}(t)+G\dot{u}(t)+(K+C)u(t)+Vu^3(t)=0 \tag{31}$$

where

$$M=(m_p+m_f)\left[\int_0^L\phi^2(x)dx-(e_oa)^2\int_0^L\phi^2(x)\frac{d^2\phi}{dx^2}dx\right]$$

$$G=\left[2m_f(1+a_kKn)\left[4\left(\frac{2-\sigma_v}{\sigma_v}\right)\left(\frac{Kn}{1+Kn}\right)+1\right]\right]\int_0^L\left[\phi(x)\left(\frac{d\phi}{dx}\right)dx-(e_oa)^2\int_0^L\phi(x)\frac{d^3\phi}{dx^3}dx\right]$$

$$K=\int_0^L(EI+E_sI_s)\phi(x)\frac{d^4\phi}{dx^4}dx+k_1\left[\int_0^L\phi^2(x)dx-(e_oa)^2\int_0^L\phi(x)\frac{d^2\phi}{dx^2}dx\right]$$

$$C=\left(\begin{array}{l}m_f\left[(1+a_kKn)\left[4\left(\dfrac{2-\sigma_v}{\sigma_v}\right)\left(\dfrac{Kn}{1+Kn}\right)+1\right]\right]^2\\+\delta A\sigma_x^o-H_s-\eta H_x^2A-k_p+\dfrac{EA\alpha\Delta T}{1-2\nu}\end{array}\right)\left[\int_0^L\phi(x)\frac{d^2\phi}{dx^2}dx-(e_oa)^2\int_0^L\phi(x)\frac{d^4\phi}{dx^4}dx\right]$$

$$V=k_3\left[\int_0^L\phi^4(x)dx-(e_oa)^2\left(3\int_0^L\phi^3(x)\frac{d^2\phi}{dx^2}dx+6\int_0^L\phi^2(x)\left(\frac{d\phi}{dx}\right)^2dx\right)\right]$$
$$+\int_0^L\phi(x)\left[\frac{EA}{2L}\int_0^L\left(\frac{d\phi}{dx}\right)^2dx\right]\frac{d^2\phi}{dx^2}dx-(e_oa)^2\int_0^L\phi(x)\left[\frac{EA}{2L}\int_0^L\left(\frac{d\phi}{dx}\right)^2dx\right]\frac{d^4\phi}{dx^4}dx$$

The circular fundamental natural frequency gives

$$\omega_n=\sqrt{\frac{K+C}{M}} \tag{32}$$

For the simply supported pipe,

$$\phi(x) = sin\beta_n x \quad (33)$$

where

$$sin\beta L = 0 \quad \Rightarrow \beta_n = \frac{n\pi}{L}$$

Eq. (31) can be written as

$$\ddot{u}(t) + \gamma\dot{u}(t) + \alpha u(t) + \beta u^3(t) = 0 \quad (34)$$

where

$$\alpha = \frac{(K+C)}{M}, \quad \beta = \frac{V}{M}, \quad \gamma = \frac{G}{M}, \quad P = \frac{F}{M}$$

For an undamped simple-simple supported structures, where $G = 0$, we have

$$\ddot{u}(t) + \alpha u(t) + \beta u^3(t) = 0 \quad (35)$$

4. Determination of Natural Frequencies

In order to determine the natural frequency of the vibration, we make use of the transformation, $\tau = \omega t$, Eq. (35) becomes

$$\omega^2\ddot{u}(\tau) + \alpha u(\tau) + \beta u^3(\tau) = 0 \quad (36)$$

The symbolic solution of Eq. (36) can be provided by assuming an initial approximation for zero-order deformation to be

$$u_o(\tau) = Acos\,\tau \quad (37)$$

Substitution of Eq. (37) into Eq. (36) provides

$$-\omega_o^2 Acos\,\tau + \alpha Acos\,\tau + \beta A^3 cos^3\tau = 0 \quad (38)$$

Through trigonometry identity, we have

$$-\omega^2 Acos\,\tau + \alpha Acos\,\tau + \beta A^3\left(\frac{3cos\,\tau + cos\,3\tau}{4}\right) = 0 \quad (39)$$

Collection of like terms gives

$$\left(\alpha A + \frac{3\beta A^3}{4} - \omega^2 A\right)cos\,\tau + \frac{1}{4}\beta A^3 cos\,3\tau = 0 \quad (40)$$

The elimination of secular term is produced by making

$$\left(\alpha A + \frac{3\beta A^3}{4} - \omega_o^2 A\right) = 0 \quad (41)$$

Therefore, the zero-order nonlinear natural frequency becomes

$$\omega_o \approx \sqrt{\alpha + \frac{3\beta A^2}{4}} \quad (42)$$

The ratio of the zero-order nonlinear natural frequency to the linear frequency

$$\frac{\omega_o}{\omega_b} \approx \sqrt{\alpha + \frac{3\beta A^2}{4}} \quad (43)$$

Similarly, the first-order nonlinear natural frequency is given as

$$\omega_1 \approx \sqrt{\frac{1}{2}\left\{\left[\alpha + \frac{3\beta A^2}{4}\right] + \sqrt{\left[\alpha + \frac{3\beta A^2}{4}\right]^2 - \left(\frac{3\beta^2 A^4}{32}\right)}\right\}} \quad (44)$$

The ratio of the first-order nonlinear natural frequency to the linear frequency

$$\frac{\omega_1}{\omega_b} \approx \sqrt{\frac{1}{2}\left\{\left[1 + \frac{3\beta A^2}{4\alpha}\right] + \sqrt{\left[1 + \frac{3\beta A^2}{4\alpha}\right]^2 - \left(\frac{3\beta^2 A^4}{32\alpha^2}\right)}\right\}} \quad (45)$$

5. The Procedure of Variation Parameter Method

The basic concept of VPM for solving differential equations is as follows: The general nonlinear equation is in the operator form

$$Lf(\eta) + Rf(\eta) + Nf(\eta) = g \quad (46)$$

The linear terms are decomposed into $L + R$, with L taken as the highest order derivative which is easily invertible and R as the remainder of the linear operator of order less than L. where g is the system input or the source term and u is the system output, Nu represents the nonlinear terms.

The VPM provides the general iterative scheme for Eq. (17) as:

$$f_{n+1}(\eta) = f_0(\eta) + \int_0^\eta \lambda(\eta,\xi)\left(-Rf_n(\xi) - Nf_n(\xi) - g(\xi)\right)d\xi \quad (47)$$

where the initial approximation $f_0(\eta)$ is given by

$$f_0(\eta) = \sum_{i=0}^{m}\frac{k_i f^i(0)}{i!} \quad (48)$$

m is the order of the given differential equation, k^i s are the unknown constants that can be determined by initial/boundary conditions and $\lambda(\eta,\xi)$ is the multiplier that reduces the order of the integration and can be determined with the help of Wronskian technique.

$$\lambda(\eta,\xi) = \sum_{i}^{m}\frac{(-1)^{i-1}\xi^{i-1}\eta^{m-1}}{(i-1)!(m-i)!} = \frac{(\eta-\xi)^{m-1}}{(m-1)!} \quad (49)$$

From the above, one can easily obtain the expressions of the multiplier for $Lf(\eta) = f^n(\eta)$

$$n=1,\quad \lambda(\eta,\xi)=1$$

$$n=2,\quad \lambda(\eta,\xi)=\eta-\xi$$

$$n=3,\quad \lambda(\eta,\xi)=\frac{\eta^2}{2!}-\eta\xi+\frac{\xi^2}{2!}$$

$$n=4,\quad \lambda(\eta,\xi)=\frac{\eta^3}{3!}-\frac{\eta^2\xi}{2!}+\frac{\eta\xi^2}{2!}-\frac{\xi^3}{3!}$$

$$n=5,\quad \lambda(\eta,\xi)=\frac{\eta^4}{4!}-\frac{\eta^3\xi}{3!}+\frac{\eta^2\xi^2}{2\cdot 2!}-\frac{\eta\xi^3}{3!}+\frac{\xi^4}{4!}$$

$$n=6,\quad \lambda(\eta,\xi)=\frac{\eta^5}{5!}-\frac{\eta^4\xi}{4!}+\frac{\eta^3\xi^2}{2\cdot 3!}-\frac{\eta^2\xi^3}{2\cdot 3!}+\frac{\eta\xi^4}{4!}-\frac{\xi^5}{5!}$$

$$n=7,\quad \lambda(\eta,\xi)=\frac{\eta^6}{6!}-\frac{\eta^5\xi}{5!}+\frac{\eta^4\xi^2}{2\cdot 4!}-\frac{\eta^3\xi^3}{6\cdot 3!}+\frac{15\eta^2\xi^4}{2\cdot 4!}-\frac{\eta\xi^5}{5!}+\frac{\xi^6}{6!}$$

$$n=8,\quad \lambda(\eta,\xi)=\frac{\eta^7}{7!}-\frac{\eta^6\xi}{6!}+\frac{\eta^5\xi^2}{2\cdot 5!}-\frac{\eta^4\xi^3}{6\cdot 4!}+\frac{\eta^3\xi^4}{6\cdot 4!}-\frac{\eta^2\xi^5}{2\cdot 5!}+\frac{\eta\xi^6}{6!}-\frac{\xi^7}{7!}$$

$$n=9,\quad \lambda(\eta,\xi)=\frac{\eta^8}{8!}-\frac{\eta^7\xi}{7!}+\frac{\eta^6\xi^2}{2\cdot 6!}-\frac{\eta^5\xi^3}{6!}+\frac{\eta^4\xi^4}{24\cdot 4!}-\frac{\eta^3\xi^5}{6!}+\frac{\eta^2\xi^6}{2\cdot 6!}-\frac{\eta\xi^7}{7!}+\frac{\xi^8}{8!}$$

$$n=10,\quad \lambda(\eta,\xi)=\frac{\eta^9}{9!}-\frac{\eta^8\xi}{8!}+\frac{\eta^7\xi^2}{2\cdot 7!}-\frac{\eta^6\xi^3}{36\cdot 5!}+\frac{\eta^5\xi^4}{24\cdot 5!}-\frac{\eta^4\xi^5}{24\cdot 5!}+\frac{\eta^3\xi^6}{36\cdot 5!}-\frac{\eta^2\xi^7}{2\cdot 7!}+\frac{\eta\xi^8}{8!}-\frac{\xi^9}{9!}$$

Consequently, an exact solution can be obtained when n approaches infinity.

Using the standard procedure of VPM as stated above, one can write the solution of Eq. (36) as

$$u_{n+1}(\tau)=a+b\tau-\frac{1}{\omega^2}\left\{\int_0^\tau(\tau-\xi)\left[\alpha u_n(\xi)+\beta u_n^3(\xi)\right]\right\}d\xi \tag{50}$$

Which can be written as

$$u_{n+1}(\tau)=u(0)+\dot{u}(0)\tau-\frac{1}{\omega^2}\left\{\int_0^\tau(\tau-\xi)\left[\alpha u_n(\xi)+\beta u_n^3(\xi)\right]\right\}d\xi \tag{51}$$

Recall that $\dot{u}(0)=0$, Therefore, Eq. (51) becomes

$$u_{n+1}(\tau)=u(0)-\left\{\frac{1}{\omega^2}\left\{\int_0^\tau(\tau-\xi)\left[\alpha u_n(\xi)+\beta u_n^3(\xi)\right]\right\}\right\}d\xi \tag{52}$$

Which can be expressed as

$$u_{n+1}(\tau)=u_0-\left\{\frac{1}{\omega^2}\left\{\int_0^\tau(\tau-\xi)\left[\alpha u_n(\xi)+\beta u_n^3(\xi)\right]\right\}\right\}d\xi \tag{53}$$

From Eq. (37), $u_o(\tau)=A\cos\tau$

$$u_{n+1}(\tau)=A\cos\tau-\left\{\frac{1}{\omega^2}\left\{\int_0^\tau(\tau-\xi)\left[\alpha u_n(\xi)+\beta u_n^3(\xi)\right]\right\}\right\}d\xi \tag{54}$$

For the first iteration

$$u_1(\tau)=A\cos\tau-\left\{\frac{1}{\omega^2}\left\{\int_0^\tau(\tau-\xi)\left[\alpha u_0(\xi)+\beta u_0^3(\xi)\right]\right\}\right\}d\xi \tag{55}$$

Which is

$$u_1(\tau)=A\cos\tau-\left\{\frac{1}{\omega^2}\left\{\int_0^\tau(\tau-\xi)\left[\alpha A\cos\xi+\beta A^3\cos^3\xi\right]\right\}\right\}d\xi \tag{56}$$

Expansion of Eq. (56) produces

$$u_1(\tau) = A\cos\tau - \left\{\frac{1}{\omega^2}\left\{\int_0^\tau \left[\alpha A\tau\cos\xi + \beta A^3\tau\cos^3\xi\right]\right\}\right\} + \left\{\frac{1}{\omega^2}\left\{\int_0^\tau \left[\alpha A\xi\cos\xi + \beta A^3\xi\cos^3\xi\right]\right\}\right\}d\xi \tag{57}$$

Using trigonometric identities, we have

$$u_1(\tau) = A\cos\tau - \left\{\frac{1}{\omega^2}\left\{\int_0^\tau \left[\alpha A\tau\cos\xi + \beta A^3\tau\left(\frac{3\cos\xi + \cos 3\xi}{4}\right)\right]\right\}\right\} + \left\{\frac{1}{\omega^2}\left\{\int_0^\tau \left[\alpha A\xi\cos\xi + \beta A^3\xi\left(\frac{3\cos\xi + \cos 3\xi}{4}\right)\right]\right\}\right\}d\xi \tag{58}$$

After integrating Eq. (58), one arrives at

$$u_1(\tau) = A\cos\tau - \frac{1}{\omega^2}\left[\alpha A\tau\sin\tau + \frac{\beta A^3\tau}{12}(9\sin\tau + \sin 3\tau)\right]$$
$$+\frac{1}{\omega^2}\left[\alpha A(\tau\sin\tau + \cos\tau - 1) + \beta A^3\left(\frac{3(\tau\sin\tau + \cos\tau - 1) + \left(\frac{\tau}{3}\sin 3\tau + \frac{1}{9}\cos 3\tau - \frac{1}{9}\right)}{4}\right)\right] \tag{59}$$

Further simplification of Eq. (59) produces

$$u_1(\tau) = A\cos\tau + \left(\frac{\alpha A}{\omega^2} + \frac{3\beta A^3}{4\omega^2}\right)(\cos\tau - 1) + \frac{\beta A^3}{36\omega^2}(\cos 3\tau - 1) \tag{60}$$

$\tau = \omega t$

Therefore, Eq. (61) can be written as

$$u_1(t) = A\cos\omega t + \left(\frac{\alpha A}{\omega^2} + \frac{3\beta A^3}{4\omega^2}\right)(\cos\omega t - 1) + \frac{\beta A^3}{36\omega^2}(\cos 3\omega t - 1) \tag{61}$$

Substitute Eqs. (33) and (61) into Eq. (29), one arrives at

$$w(x,t) = \left\{A\cos\omega t + \left(\frac{\alpha A}{\omega^2} + \frac{3\beta A^3}{4\omega^2}\right)(\cos\omega t - 1) + \frac{\beta A^3}{36\omega^2}(\cos 3\omega t - 1) + \ldots\right\}\sin\frac{n\pi x}{L} \tag{62}$$

where

$$\omega = \sqrt{\frac{1}{2}\left\{\left[\alpha + \frac{3\beta A^2}{4}\right] + \sqrt{\left[\alpha + \frac{3\beta A^2}{4}\right]^2 - \left(\frac{3\beta^2 A^4}{32}\right)}\right\}}$$

For the nonlinear free vibration of pipe conveying fluid resting on uniform foundations with damped system, we have

$$\ddot{u} + \lambda\dot{u} + \alpha u + \beta u^3 = 0 \tag{63}$$

where $\gamma = \frac{G}{M}$, but α and β have been previously defined.

One arrives at

$$\omega_{0,1th} = \sqrt{\alpha + \frac{3A^2\beta}{4}} \tag{64}$$

and

$$\omega_{0,2th} = \left[2\left(1+\frac{3A^2\beta}{4\alpha}\right)-\left(\frac{\gamma^2}{\alpha^2}\right)\right] \pm \sqrt{\left[2\left(1+\frac{3A^2\beta}{4\alpha}\right)-\left(\frac{\gamma^2}{\alpha^2}\right)\right]^2 - 4\left(1+\frac{3A^2\beta}{4\alpha}\right)^2} \tag{65}$$

Alternatively,

$$\omega_{0,2th} = \sqrt{\alpha+\frac{3A^2\beta}{4} \pm \sqrt{\frac{1}{A^2} - \lambda^2\left(\alpha+\frac{3A^2\beta}{4}\right)}} \tag{66}$$

6. Results and Discussion

In this section, the developed approximate solutions are simulated and also, the impacts of various parameters of the vibration models are developed. While Fig. 3 presents the comparison of the results of the present study with results of numerical solution using finite difference method, the effects of various parameters of the model on the dynamic response of the single-walled carbon nanotube are also presented in the figures under various subsections in the section in Figs. 4-14.

Fig. 4 illustrates the importance of surface residual stress on the vibration behaviour of the nanotube. It is shown that the dynamic response of the nanotube different for negative and positive values of surface residual stress. This establishes that the dynamic behaviour of the fluid-conveying nanotube depends on the sign of the residual surface stress. Indisputably, as it is shown in the figure, at any given adimensional amplitude, there is an increase in the frequency ratio when the negative value of the surface stress increases while the frequency ratio decreases when the positive value of the surface stress increases. This is because, the negative values of surface stress decrease the linear stiffness of the nanostructure while the positive values of surface stress increase the linear stiffness of the carbon nanotube.

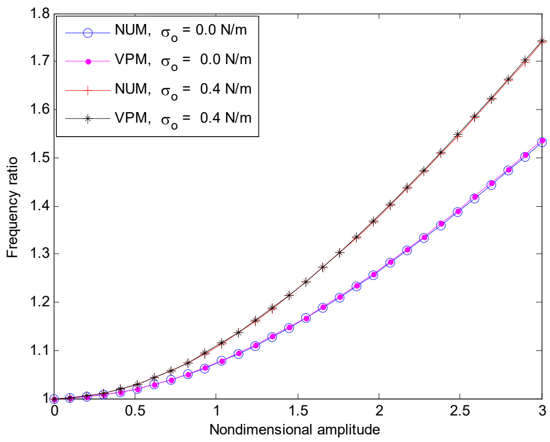

Figure 3: Comparison between the obtained results and the numerical solution for the nonlinear vibration

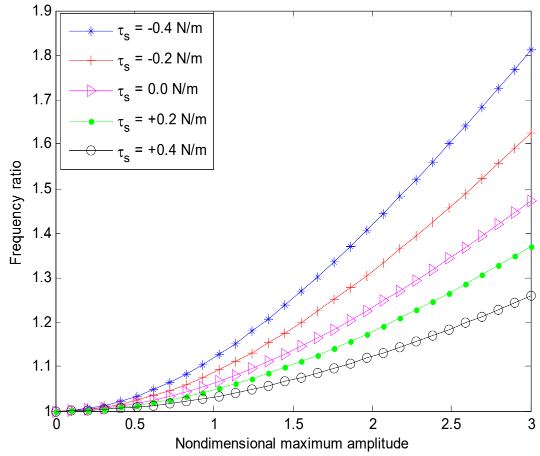

Figure 4: Effect of surface residual stress per unit length on the frequency ratio of the nanotube

Also, considering the effect of surface stress, the positive surface elasticity produces softening effect in the nanotube, while negative surface elasticity gives stiffening influence in the nanotube. Therefore, it can be stated that when the surface stress is zero, the effect of surface elasticity is not so important. Consequently, one can infer that the surface stress alone is important and effective even without consideration of the surface elasticity. However, when the surface stress is nonzero, the surface elasticity plays a significant role in the dynamic behaviour of the nanostructure.

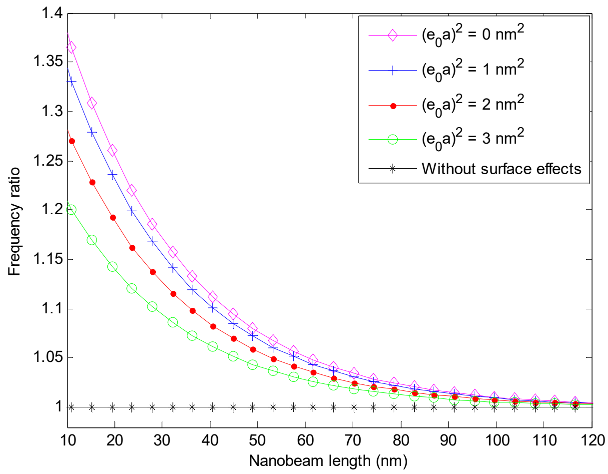

Figure5: Effects of the nanotube nonlocal parameter and length on the frequency ratio

Fig. 5 displays the significance of surface stress, nonlocality and nanobeam length on the frequency ratio of the fluid-conveying nanostructure. The figures show that the frequency ratio decreases with increase in the length and thickness ratio of the of the nanotube. It could also be stated that nonlocal parameter reduces the influence of the surface energy and stress on the frequency ratio. The results also presented that the vibration frequency of the nanotube under the consideration of the effects of surface energy and stress is larger than vibration frequency of the nanobeam given by the classical beam theory which does not consider the surface effect. Also, the figures present a clear statement that when the nanotube length increase, the natural frequency of the nanotube gradually approaches the nonlinear Euler–Bernoulli beam limit. This is as a result of decrease in the surface effect. Therefore, high thickness ratios and long nanotube length make the impacts of surface energy and stresses on the on the frequency ratio to vanish.

Fig. 6 shows the effect of initial stress on the dynamic behaviour of the nanotube. It is depicted at any adimensional amplitude increases, there is an increase in the frequency ratio as the initial stress increases.

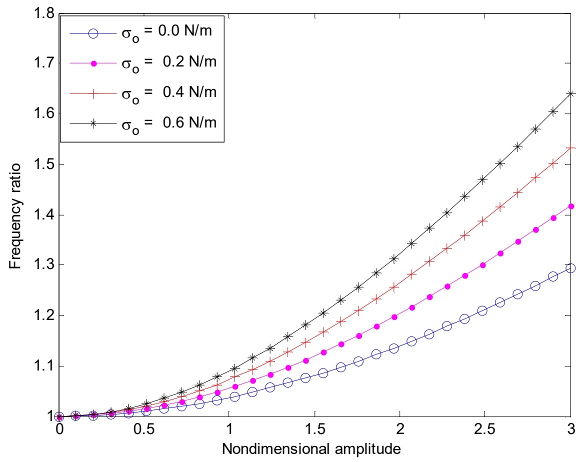

Figure 6: Effect of initial stress on the frequency ratio of the nanotube

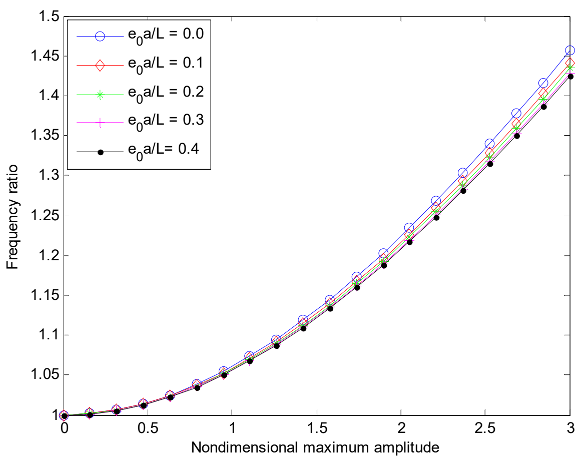

Figure 7: Effects of maximum amplitude and nonlocal parameter on ratio of the frequency ratio

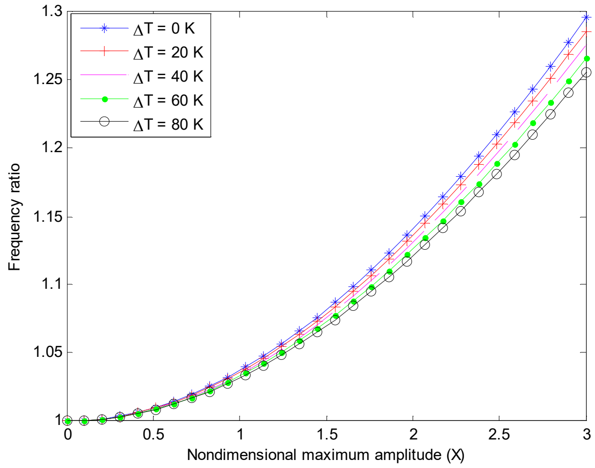

Figure 8: Effects of change in temperature on the frequency at high temperature

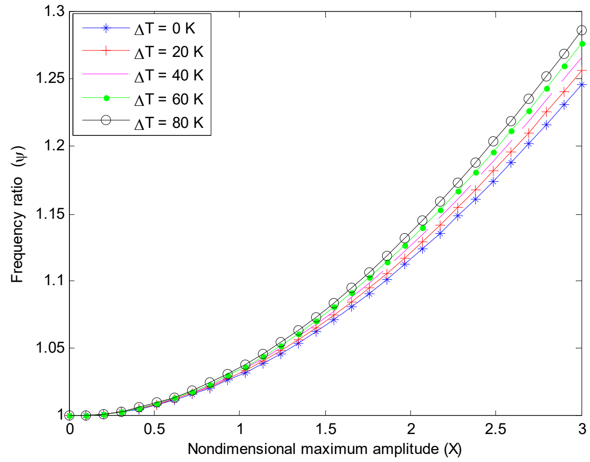

Figure 9: Effects of change in temperature on the frequency ratio at low temperature

The nonlocal parameter is a scaling parameter which makes the small-scale effect to be accounted in the analysis of microstructures and nanostructures. Fig 7 depicts the effect of the nonlocality on the frequency ratio decrease for varying adimensional amplitude. The fundamental frequency ratio of the fluid-conveying structure decreases as the nonlocal parameter increases. Also, the effect of the nonlocality on the frequency ratio decreases by increasing the amplitude ratio of the structure.

The variations in the ratio of the frequencies with adimensional nonlocal parameter for different change in temperature are presented in Figs. 8 and 9. In Fig. 8, it is shown that increase in temperature change at high temperature causes decrease in the frequency ratio. However, at room or low temperature, the frequency ratio of the hybrid nanostructure increases as the temperature change increases as shown in Fig. 8. Also, the ratio of the frequencies at low temperatures is lower than at high temperatures.

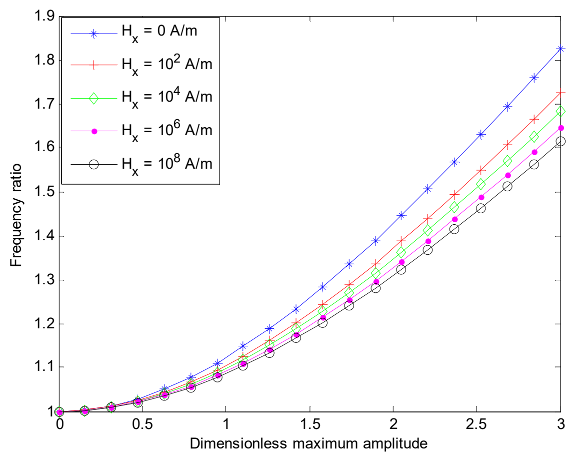

Figure 10: Effects of magnetic field strength on the frequency ratio

The effect of magnetic field strength on the frequency ratio of the nanotube is shown in Fig. 10. It is shown that the frequency ratio decreases when the strength of the magnetic field increases. Also, at high values of magnetic fields and amplitude of vibration, the discrepancy between the nonlinear and the linear frequencies increases. A further investigation shows that the vibration of the nanotube approaches linear vibration when the magnetic force strength increases to a certain high value. Such very high value of magnetic force strength which causes great attenuation in the beam can be adopted as a control and instability strategy for the nonlinear vibration system.

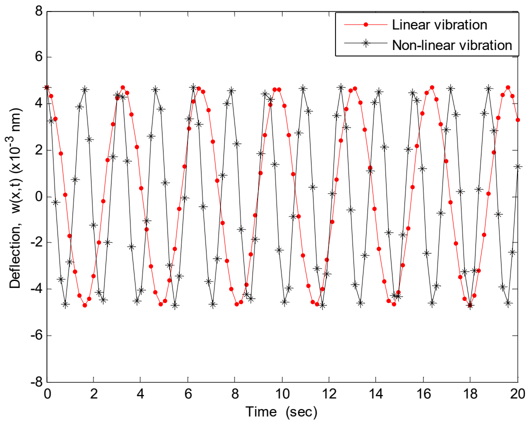

Figure 11: Linear and nonlinear dynamic behaviour of the nanostructure

Fig. 11 shows the comparison of the midpoint deflection of linear and nonlinear vibrations of the nanostructure. The nonlinear term causes stretching effect in the nonlinear in the nonlinear vibration. As stretching effect increases, the stiffness of the system increases which consequently increases in the natural frequency and the critical fluid velocity.

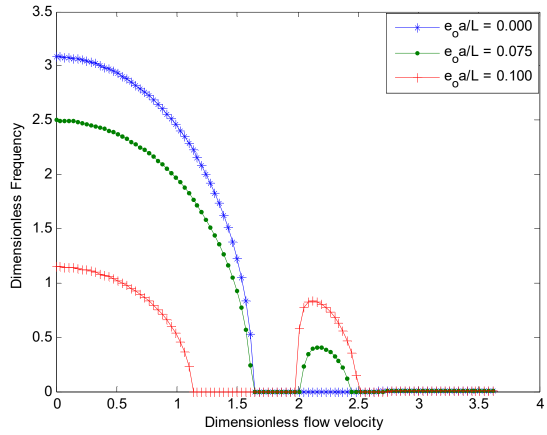

Figure 12: Effects of nonlocal parameter and fluid flow velocity on the natural frequency of the nonlinear vibration

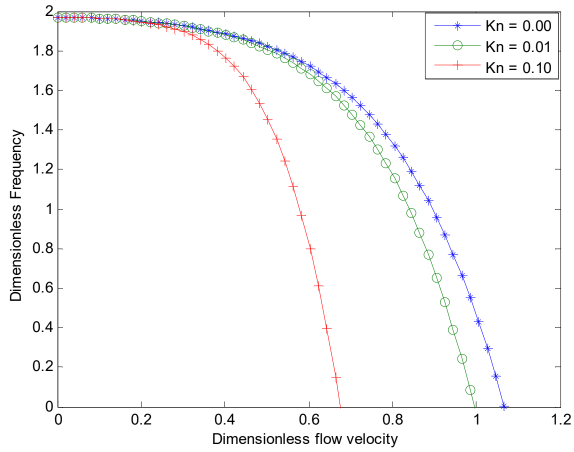

Figure 13: Effects Slip parameter (Knudsen number) on the natural frequency of the nonlinear vibration

Effects of nonlocal and slip parameters on the vibration of the nanotube is shown in Figs 12-13. It is depicted that increase in the nonlocal and slip parameters leads to decrease in the frequency of vibration and decrease in the critical velocity. Also, the Figures. depict the critical speeds corresponding to the divergence condition for different values of the system's parameters for the varying nonlocal and slip parameters.

7. Conclusion

This work has shown the potential of variation of parameter method in studying the the simultaneous impacts of surface elasticity, initial stress, residual surface tension and nonlocality on the nonlinear vibration of single-walled carbon conveying nanotube resting on linear and nonlinear elastic foundation and operating in a thermo-magnetic environment. Through the method, parametric studies were carried out and it was revealed that the ratio of the nonlinear to linear frequencies increases with the negative value of the surface stress while it decreases with the positive value of the surface stress. At any given value of nonlocal parameters, the surface effect reduces for increasing in the length of the nanotube. Also, ratio of the frequencies decreases with increase in the strength of the magnetic field, nonlocal parameter and the length of the nanotube. The natural frequency of the nanotube gradually approaches the nonlinear Euler–Bernoulli beam limit at high values of nonlocal parameter and nanotube length. It was also shown that the nonlocal parameter reduces the surface effects on the ratio of the frequencies. Further investigation shown that an increase in temperature change at high temperature causes decrease in the frequency ratio. However, at room or low temperature, the frequency ratio of the hybrid nanostructure increases as the temperature change increases. Also, the ratio of the frequencies at low temperatures is lower than at high temperatures. Lastly, it was established that an increase in the nonlocal and slip parameters leads to decrease in the frequency of vibration and decrease in the critical velocity. The present work will assist in the control and design of carbon nanotubes operating in thermo-magnetic environment and resting on elastic foundations.

Nomenclature

A	Area of the nanotube
E	Modulus of Elasticity
EI	bending rigidity
H_s	residual surface stress
H_x	magnetic field strength
I	moment of area
L	length of the nanotube
m_c	mass of tube per unit length
N	axial/Longitudinal force
T	change in temperature.
t	time coordinate
w	transverse displacement/deflection of the nanotube
W	time-dependent parameter
x	axial coordinate
$\phi(x)$	trial/comparison function
α_x	coefficient of thermal expansion
η	magnetic field permeability

References

1. Iijima, S. (1991). Helical microtubules of graphitic carbon. nature, 354(6348), 56-58.
2. Abgrall, P., & Nguyen, N. T. (2008). Nanofluidic devices and their applications. Analytical chemistry, 80(7),2326-2341.
3. Zhao, D., Liu, Y., & Tang, Y. G. (2019). Effects of magnetic field on size sensitivity of nonlinear vibration of embedded nanobeams. Mechanics of Advanced Materials and Structures, 26(11), 948-956. [4 Azrar, A., Ben Said, M., Azrar, L., & Aljinaidi, A. A. (2019). Dynamic analysis of Carbon NanoTubes conveying fluid with uncertain parameters and random excitation. Mechanics of Advanced Materials and Structures, 26(10), 898-913.
4.] Rashidi, V., Mirdamadi, H. R., & Shirani, E. (2012). A novel model for vibrations of nanotubes conveying nanoflow. Computational Materials Science, 51(1), 347-352.
5. Reddy, J. N., & Pang, S. D. (2008). Nonlocal continuum theories of beams for the analysis of carbon nanotubes. Journal of applied physics, 103(2), 023511.
6. Wang, L. (2011). A modified nonlocal beam model for vibration and stability of nanotubes conveying fluid. Physica E: Low-dimensional Systems and Nanostructures, 44(1), 25-28.
7. Lim, C. (2010). On the truth of nanoscale for nanobeams based on nonlocal elastic stress field theory: equilibrium, governing equation and static deflection. Applied Mathematics and Mechanics, 31(1), 37-54.
8. Lim, C. W., & Yang, Y. (2010). New predictions of size-dependent nanoscale based on nonlocal elasticity for wave propagation in carbon nanotubes. Journal of Computational and Theoretical Nanoscience, 7(6), 988-995.
9. Bahaadini, R., & Hosseini, M. (2016). Nonlocal divergence and flutter instability analysis of embedded fluid-conveying carbon nanotube under magnetic field. Microfluidics and nanofluidics, 20, 1-14.
10. Mahinzare, M., Mohammadi, K., Ghadiri, M., & Rajabpour, A. (2017). Size-dependent effects on critical flow velocity of a SWCNT conveying viscous fluid based on nonlocal strain gradient cylindrical shell model. Microfluidics and Nanofluidics, 21, 1-18.
11. Bahaadini, R., & Hosseini, M. (2018). Flow-induced and mechanical stability of cantilever carbon nanotubes subjected to an axial compressive load. Applied Mathematical Modelling, 59, 597-613.
12. Wang, L. (2010). Vibration analysis of fluid-conveying nanotubes with consideration of surface effects. Physica E: Low-dimensional Systems and Nanostructures, 43(1), 437-439.
13. Zhang, J., & Meguid, S. A. (2016). Effect of surface energy on the dynamic response and instability of fluid-conveying nanobeams. European Journal of Mechanics-A/Solids, 58, 1-9.
14. Hosseini, M., Bahaadini, R., & Jamali, B. (2018). Nonlocal instability of cantilever piezoelectric carbon nanotubes by considering surface effects subjected to axial flow. Journal of Vibration and Control, 24(9), 1809-1825.
15. Bahaadini, R., Hosseini, M., & Jamalpoor, A. (2017). Nonlocal and surface effects on the flutter instability of cantilevered nanotubes conveying fluid subjected to follower forces. Physica B: Condensed Matter, 509, 55-61.
16. Wang, G. F., & Feng, X. Q. (2007). Effects of surface elasticity and residual surface tension on the natural frequency of microbeams. Applied physics letters, 90(23), 231904.
17. Wang, G. F., & Feng, X. Q. (2009). Surface effects on buckling of nanowires under uniaxial compression. Applied physics letters, 94(14), 141913.
18. Farshi, B., Assadi, A., & Alinia-Ziazi, A. (2010). Frequency analysis of nanotubes with consideration of surface effects. Applied Physics Letters, 96(9), 093105.
19. Lee, H. L., & Chang, W. J. (2011). Surface effects on axial buckling of nonuniform nanowires using non-local elasticity theory. Micro & nano letters, 6(1), 19-21.
20. Lee, H. L., & Chang, W. J. (2010). Surface effects on frequency analysis of nanotubes using nonlocal Timoshenko beam theory. Journal of Applied Physics, 108(9), 093503.
21. Guo, J. G., & Zhao, Y. P. (2007). The size-dependent bending elastic properties of nanobeams with surface effects. Nanotechnology, 18(29), 295701.
22. Feng XQ, Xia R, Li XD, Li B. Surface effects on the elastic modulus of nanoporous materials. Appl Phys Lett 2009;94:011913–6.
23. He, J., & Lilley, C. M. (2008). Surface stress effect on

bending resonance of nanowires with different boundary conditions. Applied physics letters, 93(26), 263108.
24. He, J., & Lilley, C. M. (2008). Surface effect on the elastic behavior of static bending nanowires. Nano letters, 8(7), 1798-1802.
25. Jing, G. Y., Duan, H., Sun, X. M., Zhang, Z. S., Xu, J., Li, Y. D., ... & Yu, D. P. (2006). Surface effects on elastic properties of silver nanowires: contact atomic-force microscopy. Physical review B, 73(23), 235409.
26. Sharma, P., Ganti, S., & Bhate, N. (2003). Effect of surfaces on the size-dependent elastic state of nano-inhomogeneities. Applied Physics Letters, 82(4), 535-537.
27. Wang, Z. Q., Zhao, Y. P., & Huang, Z. P. (2010). The effects of surface tension on the elastic properties of nano structures. International journal of engineering science, 48(2), 140-150.
28. Selim, M. M. (2010). Torsional vibration of carbon nanotubes under initial compression stress. Brazilian Journal of Physics, 40, 283-287.
29. Cai, H., & Wang, X. (2005). Effects of initial stress on transverse wave propagation in carbon nanotubes based on Timoshenko laminated beam models. Nanotechnology, 17(1), 45.
30. Wang, X., & Cai, H. (2006). Effects of initial stress on non-coaxial resonance of multi-wall carbon nanotubes. Acta materialia, 54(8), 2067-2074.
31. Sun, C., & Liu, K. (2007). Vibration of multi-walled carbon nanotubes with initial axial loading. Solid State Communications, 143(4-5), 202-207.
32. Chen, X., Kong, T., & Wang, X. (2008). Effects of initial stress on wave propagation in multi-walled carbon nanotubes. Physica Scripta, 78(1), 015601.
33. Selim, M. M. (2010). Torsional vibration of carbon nanotubes under initial compression stress. Brazilian Journal of Physics, 40, 283-287.
34. Selim, M. (2011). Vibrational analysis of initially stressed carbon nanotubes. Acta Physica Polonica A, 119(6), 778-782.
35. Selim, M. (2011). Vibrational analysis of initially stressed carbon nanotubes. Acta Physica Polonica A, 119(6), 778-782.
36. Selim, M. M., & El-Safty, S. A. (2020). Vibrational analysis of an irregular single-walled carbon nanotube incorporating initial stress effects. Nanotechnology Reviews, 9(1), 1481-1490.
37. Eringen, A. C. (1972). Nonlocal polar elastic continua. International journal of engineering science, 10(1), 1-16.
38. Eringen, A. C. (1972). Linear theory of nonlocal elasticity and dispersion of plane waves. International Journal of Engineering Science, 10(5), 425-435.
39. Eringen, A. C. (1983). On differential equations of nonlocal elasticity and solutions of screw dislocation and surface waves. Journal of applied physics, 54(9), 4703-4710.
40. Arani, A. G., Roudbari, M. A., & Amir, S. (2016). Longitudinal magnetic field effect on wave propagation of fluid-conveyed SWCNT using Knudsen number and surface considerations. Applied Mathematical Modelling, 40(3), 2025-2038.
41. Bahaadini, R., & Hosseini, M. (2016). Effects of nonlocal elasticity and slip condition on vibration and stability analysis of viscoelastic cantilever carbon nanotubes conveying fluid. Computational Materials Science, 114, 151-159.